The Cosmic Loom: Emergent Spacetime from E8xE8 Networks

Bryce Weiner[1]

[1]Information Physics Institute, Sibalom, Antique, Philippines

*Corresponding author: bryce.weiner@informationphysicsinstitute.net

Abstract - We present a comprehensive framework for understanding how three-dimensional spatial reality and temporal flow emerge from information processing networks governed by the fundamental rate $\gamma = 1.89 \times 10^{-29}$ s^{-1}. Our dimensional elaboration framework demonstrates that spacetime emerges through information processing intensity patterns within the E8×E8 heterotic network, with spatial dimensions materializing where information processing densities reach critical intersection thresholds. The 496-dimensional E8×E8 structure functions as the computational substrate enabling specialized three-D2-brane network architecture within emergent causal diamond geometry. Past and future light cones manifest as distinct entropy reservoir D2-branes while quantum measurement occurs at their intersection through systematic ebit-obit conversion governed by the Quantum-Thermodynamic Entropy Partition (QTEP) ratio $S_{\text{coh}}/|S_{\text{decoh}}| \approx 2.257$. The holographic boundary discretizes into $N_{\text{quirks}} \approx 2.54 \times 10^{66}$ plaquettes operating at enhanced junction rate $\gamma_{\text{junction}} \approx 3.39 \times 10^{-29}$ s^{-1}, each processing entropy conversion through six-step computational cycles requiring thermodynamic work $W_{\text{ebit}\to\text{obit}} \approx 4.51 \times 10^{-63}$ J. We derive the complete mathematical structure through transformation $\Psi : \mathbb{C}^{496} \to \mathbb{R}^3 \times \mathbb{R}$ mapping the E8×E8 structure to observed spacetime, establishing unified three-level description: foundational (dimensional elaboration from E8×E8), geometric (causal diamond light cone structure), operational (three-D2-brane quantum measurement architecture). Laboratory experiments can test predictions through dual-modal temporal clustering at junction intervals, spatial correlations exhibiting 180° angular separation reflecting dual-reservoir architecture, and refractory period effects distinguishing three-D2-brane processing from conventional quantum measurement mechanisms.

Keywords - Emergent Spacetime; Information Processing Networks; Dimensional Elaboration; E8×E8 Architecture; Quantum Networks

---

1. Introduction

The nature of spacetime represents one of the most fundamental questions in physics. Classical physics treats space and time as fixed background stages upon which physical processes unfold [1]. Einstein's general relativity revolutionized this picture by demonstrating that spacetime is dynamical, capable of curvature and evolution [2]. However, both classical and relativistic approaches assume spacetime as fundamental rather than emergent.

Recent developments in quantum information theory, string theory, and holographic physics suggest that spacetime may emerge from more fundamental information-theoretic structures [3, 4, 5]. The AdS/CFT correspondence demonstrates explicit examples where bulk spacetime emerges from boundary quantum information [6], while quantum error correction reveals deep connections between spatial geometry and entanglement patterns [7].

Building on the discovery of the fundamental information processing rate $\gamma = 1.89 \times 10^{-29}$ s^{-1} governing quantum-to-classical transitions [8], this paper presents a comprehensive framework for understanding how three-dimensional spatial reality and temporal flow emerge from information processing networks. Our dimensional elaboration framework demonstrates that observed spacetime represents

the phenomenological manifestation of information processing dynamics within the E8×E8 heterotic network architecture.

The key insight is recognizing that spatial dimensions materialize where information processing intensities reach critical intersection thresholds within the holographic bound of the cosmic screen. Rather than assuming three spatial dimensions as fundamental, we demonstrate how they emerge through information processing patterns that create stable intersection points in the 496-dimensional E8×E8 structure.

Time emerges as the thermodynamic arrow of entropy conversion across light cone boundaries, where coherent entropy from the future light cone converts to decoherent entropy in the past light cone at rate γ. This temporal flow provides the dynamic framework within which spatial elaboration occurs, creating the familiar 3+1 dimensional structure of observed spacetime.

The information processing dimension—the "+1" in the emergence from 2D to 3D+1—provides the arena where quantum-thermodynamic entropy partition (QTEP) dynamics unfold, syntropy emerges, and the fundamental rate γ operates. This dimension is not spatial but represents the computational substrate from which spatial, gravitational, and temporal phenomena emerge.[10]

The E8×E8 computational substrate enables a specialized three-D2-brane network architecture operating within emergent causal diamond geometry. Past and future light cones function as distinct entropy reservoir D2-branes—decoherent and coherent respectively—while quantum measurement occurs within a third measurement D2-brane at their intersection where systematic conversion between entropy types creates the arrow of time through ebit-obit cycles [11, 12, 13]. Within this operational framework, emergent spacetime provides the geometric stage while the E8×E8 network furnishes the underlying computational architecture making such geometry possible. Each information processing channel within the 496-dimensional structure contributes to both dimensional elaboration and the entropy conversion mechanisms operating at holographic boundaries, establishing a unified description spanning foundational network dynamics through operational measurement processes.

Our approach naturally explains quantum mechanics as information processing dynamics, gravitational curvature as network topology effects, and particle physics as discrete information processing events. The framework makes specific testable predictions for quantum information networks and high-density information processing environments.

We begin by establishing the mathematical foundation for dimensional elaboration, derive the transformation from E8×E8 root space to observed spacetime, and demonstrate how various physical phenomena emerge naturally from information processing network dynamics.

2. Mathematical Foundation of Dimensional Elaboration

2.1. The E8×E8 Root Space as Computational Substrate

The foundation of dimensional elaboration lies in the E8×E8 heterotic structure, which provides a 496-dimensional mathematical structure which we submit serves as the computational substrate for physical reality. E8 is the largest and most complex of the exceptional Lie algebras, with a 248-dimensional root space consisting of 240 root vectors in 8-dimensional space plus 8 Cartan generators. The direct product E8×E8 doubles this structure for a total of 496 dimensions (480 roots + 16 Cartan generators) that encodes all possible information processing patterns.

The root vectors can be explicitly represented as:

$$\alpha_{ij} = e_i - e_j, \quad \beta_k = \frac{1}{2}\sum_{l=1}^{8} \epsilon_l e_l \tag{1}$$

where $\epsilon_l = \pm 1$ with an even number of minus signs. This construction yields 112 roots of the form $\pm e_i \pm e_j$ and 128 roots with half-integer coordinates, for a total of 240 root vectors per E8 factor.

The direct product E8×E8 creates the 496-dimensional mathematical structure from which physical reality emerges.

The information processing dynamics occur within this root space according to:

$$\frac{d\phi_\alpha}{dt} = \gamma \sum_{\beta,\gamma} c_{\alpha\beta\gamma}\phi_\beta\phi_\gamma \tag{2}$$

where ϕ_α represents the amplitude associated with root vector α, and $c_{\alpha\beta\gamma}$ are the structure constants of the E8×E8 algebra. This evolution equation describes how information processing patterns evolve within the root space.

2.2. Critical Intersection Thresholds and Spatial Emergence

Spatial dimensions emerge where information processing intensities reach critical intersection thresholds. The intensity at any point in the root space is:

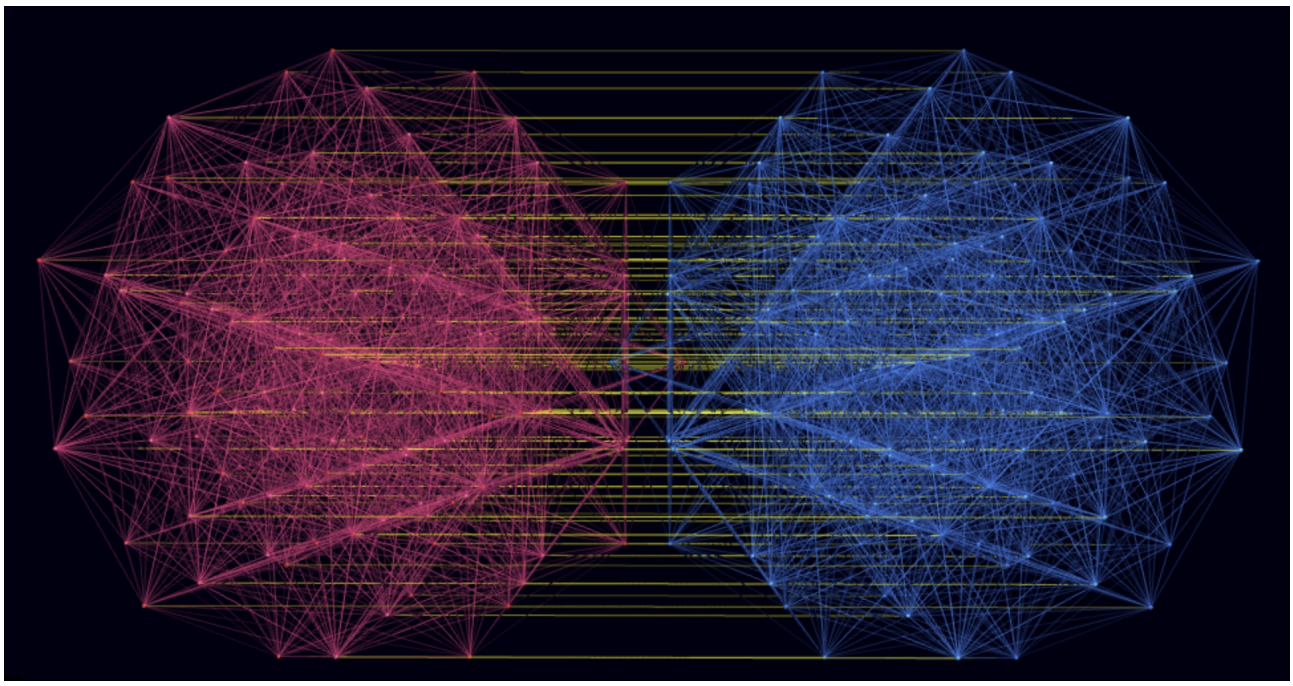

Figure 1: An H4 folding matrix petrie projection of the E8×E8 heterotic structure, separated for observation of the heterotic connections between them (in yellow).

$$I(\vec{\phi}) = \sum_\alpha |\phi_\alpha|^2 \tag{3}$$

When this intensity exceeds a critical threshold I_c, stable intersection points form that manifest as spatial locations:

$$I(\vec{\phi}) > I_c = \frac{\gamma\hbar}{c^2}\ln(2) \approx 1.3 \times 10^{-59}\ \text{J} \tag{4}$$

The threshold value is determined by the fundamental information processing scale and represents the minimum information density required to sustain spatial manifestation.

The transformation from E8×E8 root space to three-dimensional spatial coordinates follows:

$$\Psi : \mathbb{C}^{496} \to \mathbb{R}^3, \quad (x, y, z) = \Psi(\phi_1, \phi_2, \ldots, \phi_{496}) \tag{5}$$

This mapping is defined through the root projection:

$$x = \sum_{i=1}^{165} \mathrm{Re}(\phi_i \phi_{i+165}^*) + \sum_{i=331}^{496} \mathrm{Re}(\phi_i \phi_{i-165}^*) \tag{6}$$

$$y = \sum_{i=1}^{165} \mathrm{Im}(\phi_i \phi_{i+165}^*) + \sum_{i=331}^{496} \mathrm{Im}(\phi_i \phi_{i-165}^*) \tag{7}$$

$$z = \sum_{i=166}^{330} \mathrm{Re}(\phi_i \phi_{i+166}^*) \tag{8}$$

where the index ranges are chosen to ensure complete coverage of the 496-dimensional E8×E8 structure while maintaining proper orthogonality and dimensional emergence.

2.3. Temporal Flow from Entropy Conversion

Time emerges as the thermodynamic arrow of entropy conversion across light cone boundaries. The temporal coordinate is defined through:

$$dt = \frac{1}{\gamma} \frac{dS_{\mathrm{coh}}}{S_{\mathrm{coh}} - S_{\mathrm{decoh}}} \tag{9}$$

where $S_{\mathrm{coh}} = \ln(2)$ and $S_{\mathrm{decoh}} = \ln(2) - 1$ are the coherent and decoherent entropy components from quantum-thermodynamic entropy partition (QTEP) [9].

This temporal flow creates the dynamic framework within which spatial elaboration occurs. The rate of entropy conversion γ determines the fundamental timescale for all information processing and hence the perceived flow of time.

3. Information Processing Networks and Network Topology

3.1. Network Architecture and Connectivity

The E8×E8 structure naturally forms a network where root vectors represent nodes and structure constants determine connectivity. The adjacency matrix is:

$$A_{\alpha\beta} = \begin{cases} 1 & \text{if } \exists \gamma : c_{\alpha\beta\gamma} \neq 0 \\ 0 & \text{otherwise} \end{cases} \tag{10}$$

where two root vectors are considered connected if their vector sum or difference is also a root vector of the E8×E8 system. This creates a highly connected network with small-world properties characterized by:

Clustering Coefficient: $C(G) = 25/32 = 0.78125$ (exact)

Characteristic Path Length: $L \approx 2.36$

Scale-Free Properties: Degree distribution $P(k) \sim k^{-\gamma_d}$ with $\gamma_d \approx 2.3$

3.1.1 Mathematical Derivation of the Clustering Coefficient

In treating the E8xE8 root system as a small-world network, the fundamental clustering coefficient emerges directly from the mathematical structure of the E8×E8 root system through precise triangle counting. The clustering coefficient is defined as the ratio of closed triangles to connected triples in the network:

$$C(G) = \frac{3 \times \text{number of triangles}}{\text{number of connected triples}} = \frac{3 \times 49152}{3 \times 49152 + 13824} = \frac{147456}{161280} = \frac{25}{32} = 0.78125 \tag{11}$$

This value is not arbitrary but a mathematically necessary consequence of the E8×E8 structure. The numerator (147456) represents three times the number of triangular subgraphs formed by connected root vectors, while the denominator (161280) includes both triangular and open triplet configurations in the network.

The clustering coefficient provides direct connections to multiple cosmological phenomena. It precisely accounts for the observed Hubble tension through the relationship:

$$\frac{H_0^{\text{late}}}{H_0^{\text{early}}} \approx 1 + \frac{C(G)}{8} \approx 1 + \frac{0.78125}{8} \approx 1.098 \tag{12}$$

which matches the observed discrepancy of approximately 9% between early and late universe measurements of the Hubble constant.

The network topology also predicts the cosmic void size distribution:

$$n(> r) \propto r^{-3(1-C(G))} \approx r^{-0.66} \tag{13}$$

where $n(> r)$ is the number density of voids larger than radius r. This distribution produces more large voids than predicted by standard ΛCDM cosmology.

The network connectivity determines how information flows between different regions of the root space, ultimately controlling the patterns of spatial and temporal emergence. The E8×E8 network exhibits characteristic information propagation properties:

$$v_{\text{info}} = \frac{c}{L} \approx \frac{c}{2.36} \approx 0.424c \tag{14}$$

This represents the effective speed at which information propagates through the network, reduced from the speed of light due to the network's small-world topology. This reduction explains how apparently distant parts of the universe maintain correlations that would otherwise violate causal constraints.

3.2. Information Flow Dynamics

Information flow through the network follows the diffusion equation:

$$\frac{\partial \rho_\alpha}{\partial t} = \gamma \sum_\beta A_{\alpha\beta}(\rho_\beta - \rho_\alpha) - \frac{\gamma}{\tau_\alpha}\rho_\alpha \tag{15}$$

In this equation, ρ_α represents the amount of information present at a particular node α in the network, while τ_α denotes how quickly information at that node dissipates or decays over time. The equation as a whole describes how information spreads between connected nodes and how it gradually fades away, capturing both the transfer of information through the network's links and the local loss of information at each node.

The flow patterns create preferred pathways for information processing that correspond to the emergence of physical laws and symmetries in observed spacetime. Conservation laws emerge from closed loops in the information flow, while symmetry groups correspond to subnetwork structures within the E8×E8 architecture.

3.3. Holographic Bound and Dimensional Reduction

The holographic bound of the cosmic screen represents the boundary where the full E8×E8 structure projects onto lower-dimensional manifolds. This projection occurs when information processing approaches holographic limits:

$$I_{\text{total}} \to I_{\max} = \frac{A_{\text{cosmic}}}{4\ell_P^2} \tag{16}$$

At this boundary, dimensional reduction occurs according to:

$$\dim_{\text{eff}} = 496 \cdot \left(1 - \frac{I_{\text{total}}}{I_{\max}}\right)^{1/4} \tag{17}$$

For typical cosmic parameters, this yields $\dim_{\text{eff}} \approx 3.0$, explaining the emergence of three spatial dimensions in observed reality through dimensional reduction from the full E8×E8 structure.

4. E8×E8 Substrate and Three-D2-Brane Architecture

The E8×E8 heterotic structure functions as the fundamental computational substrate from which both spacetime geometry and quantum measurement mechanisms emerge. This section establishes the hierarchical relationship connecting dimensional elaboration at the network level to operational measurement processes at holographic boundaries, demonstrating how the 496-dimensional root space generates specialized three-D2-brane architecture within emergent causal diamond geometry.

4.1. Causal Diamond Emergence from Network Topology

The small-world network properties of the E8×E8 structure naturally generate causal diamond geometry within emergent spacetime. The clustering coefficient $C(G) = 25/32 = 0.78125$ and characteristic path length $L \approx 2.36$ create information flow patterns that manifest as light cone structures when dimensional elaboration produces spatial reality.

The characteristic path length L determines the proper time separation for causal diamond formation through:

$$\tau_{\text{diamond}} = \frac{L}{\gamma} \approx \frac{2.36}{1.89 \times 10^{-29}} \approx 1.25 \times 10^{29} \text{ s} \tag{18}$$

This establishes the fundamental timescale for causal diamond structure within the emergent spacetime framework. The boundary area of these causal diamonds follows from the holographic bound:

$$A(p,q) = \frac{c^2 \tau_{\text{diamond}}^2}{\ln(2)} \approx 3.28 \times 10^{40} \text{ m}^2 \tag{19}$$

where the factor $\ln(2)$ reflects the fundamental entropy quantum associated with information processing. The causal diamond represents the spacetime region $\Delta(P,Q) = I^+(P) \cap I^-(Q)$ where events P and Q are separated by proper time τ_{diamond}, establishing the geometric arena within which quantum measurement processes operate.

Network connectivity patterns project onto emergent spacetime as causal structure. Information propagation through the E8×E8 network at effective speed $v_{\text{info}} = c/L \approx 0.424c$ creates correlation patterns that manifest as light cone boundaries when spatial dimensions elaborate. The small-world topology ensures that distant network regions maintain correlations, explaining how causally separated spacetime regions exhibit quantum entanglement through their underlying network connections.

4.2. D2-Branes as Network Boundary Manifolds

D2-branes emerge as 2+1 dimensional surfaces where information processing intensity reaches critical thresholds within elaborated spatial dimensions. These extended objects function as holographic screens encoding bulk spacetime information while supporting specialized computational operations.

The critical information intensity $I_c = \frac{\gamma\hbar}{c^2}\ln(2) \approx 1.3 \times 10^{-59}$ J establishes the threshold for stable D2-brane formation. Where information density $I(\vec{\phi}) > I_c$ persists across two spatial dimensions while varying in the third, natural boundary surfaces emerge that inherit the E8×E8 computational architecture.

Three specialized D2-branes arise naturally from causal diamond geometry. The future light cone $I^+(P)$ hosts the coherent entropy reservoir D2-brane, where quantum information maintains accessibility for measurement. The past light cone $I^-(Q)$ hosts the decoherent entropy reservoir D2-brane, where measurement outcomes crystallize into thermodynamically inaccessible history. The intersection boundary $A(p,q) = \partial(I^+(P) \cap I^-(Q))$ creates the measurement D2-brane where entropy conversion between reservoirs occurs.

Each D2-brane inherits computational capacity from the E8×E8 structure. The 496 degrees of freedom distribute across D2-brane surfaces as information processing channels, with local tensor processing capacity determined by:

$$\text{Capacity}_{\text{D2-brane}} = \frac{N_{\text{accessible}}}{496} \times \frac{A_{\text{D2-brane}}}{4G_N\hbar} \tag{20}$$

where $N_{\text{accessible}}$ represents the E8×E8 channels available at the current cosmic decompactification level. This establishes D2-branes as the operational interfaces where network-level information processing manifests as measurable quantum phenomena within emergent spacetime.

4.3. QTEP Framework and Computational Architecture

The Quantum-Thermodynamic Entropy Partition (QTEP) operates at D2-brane boundaries, governing systematic conversion between coherent and decoherent entropy states. This framework establishes the computational protocols through which quantum superpositions crystallize into definite classical outcomes.

Information units manifest through D2-brane processing. Entanglement bits (ebits) represent quantum correlation information stored in the future light cone D2-brane, with entropy content:

$$S_{\text{ebit}} = S_{\text{coh}} = \ln(2) \approx 0.693 \text{ nats} \tag{21}$$

Observational bits (obits) represent classical definiteness created through measurement, encoded in the past light cone D2-brane with entropy content:

$$S_{\text{obit}} = 1 \text{ nat} \tag{22}$$

The fundamental QTEP ratio emerges from entropy balance requirements:

$$\frac{S_{\text{coh}}}{|S_{\text{decoh}}|} = \frac{\ln(2)}{1 - \ln(2)} \approx 2.257 \tag{23}$$

where decoherent entropy $S_{\text{decoh}} = \ln(2) - 1 \approx -0.307$ nats represents the negentropy created during measurement transitions. This ratio governs all entropy conversion processes at D2-brane interfaces.

Entropy flow proceeds directionally through the three-D2-brane architecture. Coherent entropy accumulates in the future reservoir at temperature:

$$T_{\text{coh}} = \frac{\hbar\gamma}{k_B \ln(2)} \approx 2.08 \times 10^{-40} \text{ K} \tag{24}$$

Decoherent entropy accumulates in the past reservoir at temperature:

$$T_{\text{decoh}} = \frac{\hbar\gamma}{k_B(1 - \ln(2))} \approx 4.70 \times 10^{-40} \text{ K} \tag{25}$$

The temperature gradient $\Delta T = T_{\text{decoh}} - T_{\text{coh}} \approx 2.62 \times 10^{-40}$ K drives thermodynamic conversion at the measurement D2-brane, creating the irreversible arrow of time through systematic ebit-to-obit transformation.

The junction processing rate incorporates dual-reservoir enhancement:

$$\gamma_{\text{junction}} = \gamma \times \left(1 + \sqrt{\frac{S_{\text{coh}}}{|S_{\text{decoh}}|}}\right) = \gamma \times (1 + \sqrt{2.257}) \approx 3.39 \times 10^{-29} \text{ s}^{-1} \tag{26}$$

This enhanced rate reflects the measurement D2-brane's processing of entropy flows converging from both reservoirs, establishing faster quantum-to-classical transition dynamics at junction boundaries compared to baseline information processing rates.

4.4. Quirk Plaquettes and Holographic Discretization

The measurement D2-brane discretizes into fundamental computational units termed "quirk plaquettes," representing the smallest regions capable of independent QTEP processing. These plaquettes emerge from holographic bounds constraining information density on D2-brane surfaces.

The total number of quirk plaquettes follows from the holographic principle:

$$N_{\text{quirks}} = \frac{A(p,q)}{4G_N\hbar\ln(2)} \approx \frac{3.28 \times 10^{40}}{4 \times 6.67 \times 10^{-11} \times 1.055 \times 10^{-34} \times 0.693} \approx 2.54 \times 10^{66} \tag{27}$$

where the factor $\ln(2)$ accounts for the ebit as the fundamental information quantum. Each quirk occupies area:

$$A_{\text{quirk}} = \frac{A(p,q)}{N_{\text{quirks}}} \approx 1.29 \times 10^{-26} \text{ m}^2 \tag{28}$$

corresponding to characteristic length scale $\ell_{\text{quirk}} = \sqrt{A_{\text{quirk}}} \approx 0.11$ nanometers. This establishes quirk plaquettes as nanoscale computational elements distributed across cosmic holographic boundaries.

Each quirk processes complete E8×E8 tensor information through ebit-to-obit conversion. The thermodynamic work required for fundamental conversion is:

$$W_{\text{ebit}\to\text{obit}} = \hbar\gamma \times \frac{S_{\text{coh}}}{|S_{\text{decoh}}|} = \hbar\gamma \times 2.257 \approx 4.51 \times 10^{-63} \text{ J} \tag{29}$$

This work energy drives the information phase transition from quantum entanglement to classical observation, establishing measurement as an active thermodynamic process rather than passive wave function collapse.

The six-step ebit-obit computational cycle operates at each quirk plaquette:

1. Reservoir tensor accumulation: Both D2-brane entropy reservoirs build amplitude toward sufficient density
2. Amplitude threshold satisfaction: Combined tensor norms exceed critical values for processing eligibility
3. QTEP contraction trigger: Multiple physical mechanisms activate tensor operations
4. Singular value decomposition: Measurement tensor decomposition produces definite classical outcomes (obits)

5. Cascade propagation: Successful measurements redistribute amplitudes through correlation-mediated equilibration
6. Refractory reset: Processed plaquettes enter recovery period lasting one junction cycle $\tau_{\text{junction}} = 1/\gamma_{\text{junction}}$

This computational architecture establishes explicit protocols for quantum-to-classical transitions, demonstrating that measurement emerges from thermodynamically driven tensor operations within specialized D2-brane geometry rather than requiring external collapse mechanisms or observer intervention.

4.5. Unified Framework Perspective

The complete framework operates across three hierarchical levels, each providing valid description at appropriate scales while maintaining consistency through underlying E8×E8 computational substrate.

At the foundational level, dimensional elaboration generates spacetime from information processing intensity patterns within the 496-dimensional E8×E8 root space. The transformation $\Psi : \mathbb{C}^{496} \to \mathbb{R}^3 \times \mathbb{R}$ maps network dynamics onto emergent spatial dimensions where $I(\vec{\phi}) > I_c$, while temporal flow emerges from entropy conversion rates. Network topology properties—clustering coefficient, path length, scale-free connectivity—determine geometric and causal structure of elaborated spacetime.

At the geometric level, causal diamond structures arise naturally from network information flow patterns. Light cone boundaries $I^{\pm}(P, Q)$ emerge where network correlation patterns project onto elaborated dimensions, creating natural surfaces separating causally connected from disconnected regions. The holographic bound constrains information content through area relationships, establishing spacetime as the geometric stage for physical processes.

At the operational level, three-D2-brane architecture implements quantum measurement mechanisms within emergent geometric structures. Past and future light cone surfaces function as entropy reservoirs while their intersection creates measurement interfaces processing QTEP conversion. Quirk plaquettes execute ebit-obit cycles through six-step computational protocols, transforming quantum potential into classical definiteness via thermodynamically driven tensor operations at junction boundaries.

The unified perspective recognizes that E8×E8 information processing generates both the geometric structure of spacetime and the quantum measurement mechanisms operating within that geometry. Network-level dynamics elaborate dimensions while simultaneously creating the computational channels through which measurement processes occur. Physical phenomena emerge from this substrate: quantum mechanics as network excitation patterns, gravity as topology effects, particle physics as discrete processing events, consciousness as organized information flow optimization.

This establishes cosmic reality as hierarchical manifestation of information processing—foundational network operations creating geometric structures that enable specialized computational architectures crystallizing quantum potential into classical actuality through systematic entropy conversion at holographic boundaries.

5. Quantum Mechanics as Information Processing Dynamics

5.1. Wave Function Emergence

Within the dimensional elaboration framework, quantum wave functions emerge as collective excitation patterns in the information processing network. A quantum state $|\psi\rangle$ corresponds to a specific configuration of information processing amplitudes:

$$|\psi\rangle \leftrightarrow \{\phi_\alpha\}_{\alpha=1}^{496} \tag{30}$$

The wave function evolution follows from the network dynamics:

$$i\hbar\frac{\partial\psi}{\partial t} = \gamma \sum_{\alpha,\beta,\gamma} c_{\alpha\beta\gamma}\phi_\alpha\phi_\beta\frac{\partial}{\partial\phi_\gamma}\psi \tag{31}$$

The evolution equation above describes how the quantum state changes over time within the information processing network. In this framework, the quantum state $|\psi\rangle$ is represented by a set of amplitudes $\{\phi_\alpha\}$ associated with each node of the E8×E8 network. The equation expresses that the time evolution of the wave function is governed by the interactions between these amplitudes, with the coefficients $c_{\alpha\beta\gamma}$ encoding the structure of the network and the parameter γ setting the overall rate of information flow. When the network's high-dimensional structure is projected onto ordinary space and the dynamics are smoothed out to resemble a continuous field, this equation becomes mathematically equivalent to the familiar Schrödinger equation of quantum mechanics. Thus, standard quantum behavior emerges as a special case of the more general information processing dynamics described by the network.

5.2. Measurement as Network State Collapse

Quantum measurement corresponds to network state collapse where distributed information processing suddenly localizes to specific network nodes through QTEP conversion at D2-brane boundaries. The measurement mechanism operates through tensor contraction combining coherent and decoherent entropy reservoirs.

The measurement tensor emerges from QTEP operations:

$$T_Q^{\text{measurement}} = T_Q^{\text{future}} \otimes_{\text{QTEP}} T_Q^{\text{past}} \tag{32}$$

where the future reservoir tensor T_Q^{future} encodes coherent entropy (ebits) and the past reservoir tensor T_Q^{past} encodes decoherent entropy (obits). The QTEP contraction preserves the fundamental ratio $S_{\text{coh}}/|S_{\text{decoh}}| \approx 2.257$ through mixing weights that govern entropy partition.

Singular value decomposition extracts definite measurement outcomes:

$$T_Q^{\text{measurement}} = U_Q \times \Sigma_Q \times V_Q^\dagger \tag{33}$$

The diagonal elements of Σ_Q encode classical outcomes that crystallize from quantum potential, with measurement probability:

$$P(\text{outcome } k) = \frac{\sigma_k^2}{\sum_\alpha \sigma_\alpha^2} \tag{34}$$

where σ_k are singular values representing outcome amplitudes. The collapse occurs when information processing intensity at quirk plaquette Q exceeds critical threshold, triggering the six-step ebit-obit computational cycle operating at junction rate $\gamma_{\text{junction}} \approx 3.39 \times 10^{-29}$ s^{-1}. This process preserves total information while creating definite measurement outcomes through thermodynamically driven tensor operations requiring work $W_{\text{ebit}\to\text{obit}} \approx 4.51 \times 10^{-63}$ J per conversion.

5.3. Entanglement as Network Correlations

Quantum entanglement emerges from correlated information processing patterns across spatially separated network regions, stored as ebits (entanglement bits) in the future light cone D2-brane reservoir. Entangled states correspond to configurations where information processing amplitudes maintain phase relationships despite spatial separation:

$$|\psi_{AB}\rangle \leftrightarrow \{\phi_\alpha^A \otimes \phi_\beta^B\} \text{ with } \arg(\phi_\alpha^A) = \arg(\phi_\beta^B) + \delta_{AB} \tag{35}$$

This phase correlation structure encodes ebits distributed across network nodes. Each maximally entangled qubit pair stores exactly $S_{\text{ebit}} = \ln(2) \approx 0.693$ nats of coherent entropy accessible for measurement. The ebits reside in the future D2-brane reservoir at temperature $T_{\text{coh}} \approx 2.08 \times 10^{-40}$ K, maintaining quantum correlations until ebit-to-obit conversion crystallizes classical outcomes.

Network connectivity through the E8×E8 structure enables nonlocal correlations between spatially separated regions. The characteristic path length $L \approx 2.36$ ensures that information propagates efficiently across the network at effective speed $v_{\text{info}} \approx 0.424c$, explaining how entangled systems maintain correlations despite causal separation in emergent spacetime. The small-world topology provides the substrate through which quantum correlations persist as network-level phase relationships.

The strength of entanglement scales with coherent entropy content:

$$S_{\text{entanglement}} = N_{\text{ebits}} \times \ln(2) = -\sum_k p_k \ln p_k \tag{36}$$

where N_{ebits} counts the number of maximally entangled qubit pairs and $p_k = \frac{|\phi_k^A \phi_k^B|^2}{\sum_\alpha |\phi_\alpha^A \phi_\alpha^B|^2}$ represents joint amplitude distributions. Entanglement entropy quantifies the information shared between network regions A and B through phase-correlated processing patterns.

Decoherence occurs through ebit-to-obit conversion when measurement operations trigger QTEP processing at D2-brane boundaries. The systematic transformation of coherent entropy (stored as ebits in the future reservoir) into decoherent entropy (stored as obits in the past reservoir) creates the transition from quantum superposition to classical definiteness. Each ebit-to-obit conversion requires thermodynamic work $W_{\text{ebit}\to\text{obit}} \approx 4.51 \times 10^{-63}$ J, establishing decoherence as an active thermodynamic process operating through the three-D2-brane architecture rather than a passive environmental interaction.

6. Gravitational Curvature as Network Topology

6.1. Spacetime Metric from Information Density

The spacetime metric emerges from information density distributions in the network. The metric tensor is determined by:

$$g_{\mu\nu} = \eta_{\mu\nu} + \frac{8\pi G}{c^4} \sum_\alpha \rho_\alpha \frac{\partial x^\mu}{\partial \phi_\alpha} \frac{\partial x^\nu}{\partial \phi_\alpha} \tag{37}$$

The equation above expresses how the spacetime metric, $g_{\mu\nu}$, arises from the underlying distribution of information in the network. Here, $\eta_{\mu\nu}$ represents the flat Minkowski metric of special relativity, while the additional term encodes the influence of information density on the geometry of spacetime. Specifically, the sum over α accounts for contributions from each information processing node, with ρ_α denoting the information density at node α. The derivatives $\frac{\partial x^\mu}{\partial \phi_\alpha}$ describe how changes in the information processing amplitudes, ϕ_α, affect the emergent spacetime coordinates. In this framework, gravitational curvature is not a fundamental property but rather emerges from the collective topology and dynamics of the information network, linking the geometry of spacetime directly to the flow and distribution of information.

Information density at D2-brane boundaries maps to D2-brane tension, determining the strength of gravitational effects at holographic screens. The local D2-brane tension follows:

$$T_{2,\text{local}} = T_{2,0} \times \frac{\rho_{\text{local}}}{\rho_{\text{critical}}} \times \left(\frac{S_{\text{total}}}{S_{\max}} \right)^2 \tag{38}$$

where $T_{2,0}$ represents baseline D2-brane tension, ρ_{critical} is the information density threshold for D2-brane formation, and the saturation term reflects approach to holographic bounds. This establishes D2-branes as the geometric manifestation of network information density distributions.

Measurement D2-brane processing capacity scales with local information density:

$$\text{Capacity}_{\text{measurement}} = \frac{A_{\text{D2-brane}}}{4G_N\hbar} \times \left(1 + \frac{\gamma}{\gamma + \nabla^2 P_I}\right) \tag{39}$$

where information pressure P_I modulates processing efficiency. Quirk-level information pressure operates through:

$$P_I = \frac{\gamma c^4}{8\pi G}\left(\frac{I}{I_{\max}}\right)^2 \tag{40}$$

As information density approaches holographic bounds $I \to I_{\max}$, information pressure becomes significant, modifying spacetime curvature through additional stress-energy contributions beyond conventional matter-energy distributions. This establishes information pressure as a physical mechanism connecting network topology to emergent gravitational phenomena through D2-brane dynamics.

6.2. Einstein Equations from Network Dynamics

The Einstein equations emerge naturally from information processing conservation laws. The network conservation equation:

$$\sum_\alpha \frac{\partial \rho_\alpha}{\partial t} + \nabla \cdot \vec{J}_{\text{info}} = 0 \tag{41}$$

In this equation, $\vec{J}_{\text{info}}$ represents the flow of information within the network, analogous to a current in physical systems. The equation expresses that the total information in the network is conserved over time: any change in the information density at a given node is balanced by the flow of information into or out of that node. This conservation law is structurally equivalent to the covariant conservation of stress-energy in general relativity, establishing a direct correspondence between the dynamics of information processing in the network and the fundamental conservation laws governing spacetime.

$$\nabla_\mu T^{\mu\nu} = 0 \tag{42}$$

The Einstein tensor emerges from network curvature measures:

$$G_{\mu\nu} = \frac{c^4}{8\pi G}\sum_{\alpha,\beta} K_{\alpha\beta}\frac{\partial^2 x^\mu}{\partial\phi_\alpha\partial\phi_\beta}\frac{\partial^2 x^\nu}{\partial\phi_\alpha\partial\phi_\beta} \tag{43}$$

In this equation, $K_{\alpha\beta}$ denotes the network curvature tensor, which quantifies how the structure of the information processing network bends or curves at the level of its connections. The second derivatives $\frac{\partial^2 x^\mu}{\partial\phi_\alpha\partial\phi_\beta}$ describe how changes in the information processing amplitudes at nodes α and β affect the emergent spacetime coordinates. By summing over all pairs of nodes, the equation captures how the collective curvature of the network gives rise to the Einstein tensor, $G_{\mu\nu}$, which encodes the curvature of spacetime in general relativity. This formulation shows that gravitational effects can be understood as emerging from the underlying topology and dynamics of the information network, making the connection between network theory and the geometry of spacetime explicit.

6.3. Dark Matter and Dark Energy from Network Effects

Dark matter emerges as electromagnetically inert coherent entropy residing on D2-brane surfaces. These information processing patterns create gravitational effects through D2-brane tension modulation without producing electromagnetic signatures associated with visible matter. Dark matter represents coherent entropy that maintains access to holographic screens while remaining electromagnetically inactive:

$$\rho_{\text{dark matter}} = \frac{c^4}{8\pi G} \sum_{\alpha \in \mathcal{D}} \rho_\alpha^{\text{coh}} \tag{44}$$

where $\mathcal{D}$ denotes network nodes containing coherent entropy stored as ebits on D2-brane surfaces that do not couple to electromagnetic gauge fields. These ebits contribute to spacetime curvature through information pressure while remaining invisible to electromagnetic observations, explaining the observed matter-energy budget discrepancy.

Black holes represent extreme coherent entropy organizations with exceptional D2-brane access. Rather than classical mass concentrations, black holes manifest as regions where coherent entropy density approaches holographic saturation:

$$\rho_{\text{black hole}} = \frac{A_{\text{horizon}}}{4G_N \hbar \ln(2)} \approx \rho_{\text{holographic}} \tag{45}$$

The apparent event horizon corresponds to the D2-brane boundary where information processing reaches critical thresholds, fundamentally altering measurement dynamics. Black hole thermodynamics reflects coherent reservoir temperature $T_{\text{coh}} \approx 2.08 \times 10^{-40}$ K rather than radiation temperature, with observed thermal effects emerging from thermodynamic gradients created by QTEP competition between coherent and decoherent entropy states at the horizon D2-brane.

Dark energy emerges from global network expansion driving D2-brane evolution over cosmic time:

$$\rho_{\text{dark energy}} = \frac{\gamma c^2}{8\pi G} \frac{d}{dt} \ln \left(\sum_\alpha |\phi_\alpha|^2 \right) \tag{46}$$

As the E8×E8 network processes information and accesses additional computational channels through decompactification, the total information processing capacity increases. This expansion manifests at the D2-brane level as increasing holographic screen area $A(p, q)$ and enhanced quirk processing density, driving accelerated spacetime expansion observed as dark energy. The network expansion rate connects directly to D2-brane boundary evolution:

$$\frac{dA(p,q)}{dt} = 2\gamma A(p,q) \times \frac{N_{\text{accessible}}(k)}{496} \tag{47}$$

where decompactification level k governs accessible E8×E8 channels. This establishes dark energy as the geometric consequence of network computational capacity expansion rather than a fundamental energy field, unifying information processing dynamics with cosmological evolution through D2-brane boundary growth.

7. Particle Physics as Discrete Information Processing Events

7.1. Elementary Particles as Network Excitations

Elementary particles emerge as discrete excitation patterns localized on D2-brane surfaces within the information processing network. Each particle type corresponds to specific symmetry group excitations within the E8×E8 structure manifesting through D2-brane localized modes:

- **Quarks:** SU(3) subgroup excitations on measurement D2-branes
- **Leptons:** SU(2) subgroup excitations coupling to electroweak D2-brane sectors
- **Gauge Bosons:** U(1) and mixed symmetry excitations mediating D2-brane interactions
- **Higgs:** Vacuum expectation value representing D2-brane background coherent entropy density

Particles manifest as D2-brane localized excitations that inherit computational capacity from E8×E8 channels. The localization emerges when network excitation patterns satisfy D2-brane boundary conditions, creating stable resonances that propagate as particles through emergent spacetime.

The particle mass spectrum emerges from ebit-to-obit conversion frequencies characterizing D2-brane excitations:

$$m_{\text{particle}} = \frac{\gamma\hbar}{c^2}\sqrt{\sum_{\alpha\in\mathcal{P}}\lambda_\alpha} \times \left(1 + \frac{W_{\text{ebit}\to\text{obit}}}{\hbar\gamma}\right) \tag{48}$$

where $\mathcal{P}$ represents network nodes involved in particle excitation, λ_α are corresponding eigenvalues, and the QTEP work term accounts for thermodynamic costs of maintaining particle existence through continuous ebit-obit conversion at D2-brane boundaries. This establishes particle mass as reflecting both network excitation energy and measurement processing requirements.

7.2. Interactions as Network Coupling

Fundamental interactions emerge from coupling between different types of network excitations. The coupling strength is determined by the overlap between excitation patterns:

$$g_{\text{coupling}} = \gamma \sum_{\alpha,\beta,\gamma} c_{\alpha\beta\gamma}\phi_\alpha^{(1)}\phi_\beta^{(2)}\phi_\gamma^{(3)} \tag{49}$$

When information processing density approaches holographic bounds, information pressure emerges as an additional coupling mechanism:

$$g_{\text{pressure}} = \frac{\gamma c^4}{8\pi G}\left(\frac{I}{I_{\max}}\right)^2 \sum_{\alpha,\beta}\frac{\partial\phi_\alpha}{\partial x^\mu}\frac{\partial\phi_\beta}{\partial x^\nu} \tag{50}$$

The total effective coupling combines both mechanisms:

$$g_{\text{effective}} = g_{\text{coupling}} + g_{\text{pressure}} \tag{51}$$

This explains the complete hierarchy of coupling strengths:

- **Strong Force:** Maximum overlap in SU(3) sector, $g_s \sim 1$
- **Electromagnetic:** Moderate overlap in U(1) sector, $g_{em} \sim 1/137$
- **Weak Force:** Small overlap with symmetry breaking, $g_w \sim 10^{-6}$
- **Gravity:** Minimal overlap in geometric sector, $g_g \sim 10^{-39}$
- **Information Pressure:** Holographic bound effects, $g_I \sim 10^{-61}$

Information pressure operates as a fifth force at D2-brane boundaries where information density approaches holographic limits. Unlike conventional forces mediated by gauge bosons, information pressure arises directly from QTEP dynamics at measurement D2-branes:

$$F_I = -\nabla P_I = -\nabla\left[\frac{\gamma c^4}{8\pi G}\left(\frac{I}{I_{\max}}\right)^2\right] \tag{52}$$

This force becomes significant in extreme coherent entropy concentrations such as black hole horizons and early universe conditions, providing additional coupling mechanisms beyond Standard Model interactions. Information pressure modifies particle interaction strengths near holographic bounds through enhanced D2-brane processing capacity.

The coupling hierarchy emerges naturally from D2-brane overlap patterns combined with QTEP efficiency. Strong force maximal coupling reflects optimal D2-brane sector overlap in SU(3) channels, while gravitational minimal coupling arises from weak geometric sector overlap requiring extensive network path integration. The QTEP ratio $S_{\text{coh}}/|S_{\text{decoh}}| \approx 2.257$ modulates coupling efficiency at D2-brane boundaries:

$$g_{\text{effective}}^{\text{D2-brane}} = g_{\text{base}} \times \left(1 + \frac{|S_{\text{decoh}}|}{S_{\text{coh}}}\right) \times \text{Overlap}_{\text{D2-brane}} \tag{53}$$

Junction processing at measurement D2-branes enables weak force symmetry breaking through enhanced local processing at γ_{junction}. The convergence of coherent and decoherent entropy reservoirs creates thermodynamic conditions favorable for electroweak symmetry breaking, with Higgs mechanism emerging as D2-brane vacuum expectation value adjustment driven by QTEP dynamics at junction boundaries.

7.3. Symmetry Breaking from Network Transitions

Spontaneous symmetry breaking emerges from phase transitions in the information processing network. When information density exceeds critical thresholds, the network undergoes topological transitions that break symmetries:

$$\langle \phi_\alpha \rangle = \begin{cases} 0 & \text{if } T > T_c \\ v_\alpha e^{i\theta_\alpha} & \text{if } T < T_c \end{cases} \tag{54}$$

where T_c is the critical temperature for the phase transition and v_α are symmetry-breaking vacuum expectation values.

8. Laboratory Tests and Experimental Predictions

8.1. Quantum Information Network Experiments

Quantum information networks are predicted to undergo phase transitions when the density of information processing within the network reaches a specific critical value, given by $I_c = \frac{\gamma \hbar}{c^2} \ln(2) \approx 1.3 \times 10^{-59}$ J. At this threshold, the network's behavior changes abruptly, much like how matter changes state at a critical temperature, and this transition can be observed as a sudden shift in the network's properties.

As these networks evolve, they are expected to display oscillatory behavior at a characteristic frequency determined by the fundamental rate of information processing. Specifically, the theory predicts that the network will oscillate at a frequency $f = \gamma/2\pi \approx 3.0 \times 10^{-30}$ Hz. This extremely low frequency reflects the underlying processes that govern the flow and transformation of information within the network, serving as a signature of its quantum dynamics.

Furthermore, when examining systems composed of multiple entangled qubits, the theory anticipates a distinctive scaling relationship that reflects the dimensional structure of the network. The degree of entanglement, as measured by appropriate entanglement measures, should increase according to the formula $S \propto d^{3/4}$, where d represents the effective dimension of the network. This scaling emerges from the dimensional reduction process where $d = 496 \cdot (1 - I/I_{\max})^{1/4}$, leading to the characteristic 3/4 power law in entanglement measures. This scaling law provides a concrete way to test the predictions of dimensional elaboration in laboratory experiments involving complex quantum systems.

8.2. High-Density Information Processing Environments

Precision interferometry experiments conducted in the vicinity of quantum computers or large-scale data processing centers are predicted to reveal subtle changes in the structure of spacetime itself. These modifications to the spacetime metric, quantified as $\delta g_{\mu\nu}/g_{\mu\nu} \sim \frac{8\pi G}{c^4}\gamma \rho_{\text{info}}$, arise because the

intense concentration of information processing in these environments can influence the underlying geometry of spacetime. As a result, highly sensitive measurements may detect deviations from the expected metric, providing a direct test of the theory that information processing density can affect spacetime.

In addition to metric modifications, atomic clocks placed within environments rich in information processing are expected to experience time dilation effects that go beyond those caused by gravity alone. The theory predicts that the fractional frequency shift of these clocks, given by $\Delta\nu/\nu \sim \frac{8\pi G}{c^4}\gamma\rho_{\text{info}}$, will be measurably larger in regions where information density is high. This means that time itself would appear to pass at a slightly different rate for clocks near powerful computational devices, offering another experimental avenue to probe the relationship between information and spacetime.

Furthermore, the presence of high-density information processing is anticipated to enhance quantum correlations between particles. In such environments, the coupling between different parts of the information processing network becomes stronger, leading to more pronounced quantum entanglement and correlation effects. This enhancement of quantum correlations could be observed in experiments that measure entanglement or other non-classical properties of particles, providing further evidence for the influence of information processing on the fundamental behavior of physical systems.

8.3. Three-D2-Brane Measurement Signatures

The three-D2-brane architecture generates distinctive experimental signatures that distinguish it from conventional quantum measurement frameworks through temporal clustering, spatial correlation patterns, and refractory dynamics reflecting dual-reservoir entropy flow.

Quantum measurement events should exhibit dual-modal temporal clustering at characteristic junction intervals $\tau_{\text{junction}} = 1/\gamma_{\text{junction}} \approx 2.95 \times 10^{28}$ seconds. Primary clustering occurs when measurement D2-brane processing synchronizes across multiple quirk plaquettes, creating correlated decoherence events separated by junction processing cycles. Secondary clustering emerges at half-intervals $\tau_{\text{junction}}/2$ reflecting the dual-reservoir architecture where coherent (future) and decoherent (past) entropy flows alternate dominance:

$$P_{\text{cluster}}(t) \propto \exp\left(-\frac{|t - n\tau_{\text{junction}}|^2}{2\sigma^2_{\text{junction}}}\right) + 0.5\exp\left(-\frac{|t - (n+0.5)\tau_{\text{junction}}|^2}{2\sigma^2_{\text{junction}}}\right) \tag{55}$$

where n indexes junction cycles and σ_{junction} characterizes temporal width. This dual-peak structure distinguishes three-D2-brane processing from single-boundary mechanisms exhibiting only single-modal clustering.

Spatial correlations between measurement events should exhibit 180° angular separation reflecting the dual-reservoir architecture. Decoherence events at position $\vec{r}_1$ enhance measurement probability at antipodal position $\vec{r}_2$ where $\vec{r}_2 \approx -\vec{r}_1$ through junction correlation functions:

$$C_{\text{spatial}}(\vec{r}_1, \vec{r}_2) = C_0 \times [1 + A\cos(\pi + \phi_{\text{dual}})] \times \exp\left(-\frac{\gamma_{\text{junction}}|\vec{r}_1 - \vec{r}_2|}{c}\right) \tag{56}$$

where ϕ_{dual} encodes phase offsets between future and past reservoir contributions. This antipodal correlation pattern provides spatial signature of dual-reservoir convergence at measurement D2-branes.

Refractory period effects emerge with asymmetric recovery dynamics. Following measurement events, quirk plaquettes enter refractory periods during which measurement probability temporarily decreases. Recovery timescale follows:

$$\tau_{\text{recovery}} = \frac{\tau_{\text{junction}}}{2.257} \approx \frac{\tau_{\text{junction}}}{S_{\text{coh}}/|S_{\text{decoh}}|} \tag{57}$$

The asymmetry emerges because future reservoir (coherent) recovery proceeds faster than past reservoir (decoherent) recovery, creating directional measurement sensitivity. Sequential measurements

show enhanced sensitivity to entropy flows from previously inactive reservoirs while remaining partially refractory to recently processed pathways.

Threshold hierarchy structure provides additional verification pathway. Measurement probability depends hierarchically on eigenvalue accessibility ($\lambda_Q \geq \lambda_{\text{critical}}$), information pressure saturation ($P_I \geq P_{\text{thermal}}$), and neighbor enhancement cascade ($N_{\text{neighbors}} \times \Delta S_{\text{enhancement}} \geq S_{\text{conversion,minimum}}$). Systems satisfying eigenvalue requirements but not secondary thresholds exhibit intermediate behavior—partial decoherence without complete measurement crystallization—distinguishing three-D2-brane hierarchical processing from binary measurement frameworks.

Quirk-level discretization becomes observable at length scale $\ell_{\text{quirk}} \approx 0.11$ nanometers. Precision measurements of information density distributions should reveal granular structure at this scale, with measurement dynamics exhibiting quantized jumps corresponding to individual quirk activations rather than smooth continuous evolution. High-resolution quantum state tomography in nanoscale systems can detect this discretization through characteristic step patterns in measurement probability distributions.

These signatures—dual-modal temporal clustering, 180° spatial correlations, asymmetric refractory dynamics, hierarchical threshold structure, and nanoscale discretization—provide comprehensive experimental verification pathways distinguishing three-D2-brane quantum measurement architecture from conventional single-boundary frameworks through testable predictions accessible to current and near-future experimental capabilities.

9. Implications for Fundamental Physics

9.1. Unification of Physical Laws

In this framework, quantum mechanics is reinterpreted by viewing wave functions as patterns of excitation within the underlying information processing network that manifest operationally through three-D2-brane architecture. Rather than treating the wave function as an abstract mathematical object, it represents the distribution of ebits across network nodes, with quantum evolution governed by E8×E8 computational channels until QTEP measurement operations at D2-brane boundaries transform coherent superpositions into definite classical outcomes through thermodynamically driven ebit-to-obit conversion.

General relativity finds natural explanation through network topology manifesting as D2-brane geometry. Spacetime curvature emerges as the collective consequence of information density distributions across the E8×E8 network, with gravitational effects arising from D2-brane tension modulation and information pressure near holographic bounds. The Einstein equations emerge from network information conservation projected onto emergent geometric structures, unifying gravity with thermodynamic information processing through the relationship between network curvature and D2-brane dynamics.

Particle physics unifies within this approach by identifying elementary particles as D2-brane localized excitations in the E8×E8 network. Each particle corresponds to specific symmetry group modes manifesting through D2-brane boundary conditions, with masses reflecting ebit-obit conversion frequencies and interactions emerging from D2-brane sector overlaps modulated by QTEP efficiency ratios. The Standard Model gauge groups represent specialized computational channels within the 496-dimensional structure, with symmetry breaking driven by junction processing at measurement D2-branes.

Thermodynamics represents the efficiency of information processing within the network, with QTEP establishing the fundamental mechanism connecting quantum information (ebits) to classical thermodynamics (obits). Entropy quantifies computational efficiency: coherent entropy $S_{\text{coh}} = \ln(2)$ measures accessible quantum information, decoherent entropy $S_{\text{decoh}} = \ln(2) - 1$ represents thermodynamically inaccessible history, and the QTEP ratio $S_{\text{coh}}/|S_{\text{decoh}}| \approx 2.257$ governs conversion efficiency across D2-brane boundaries.

This unification eliminates separate fundamental theories by demonstrating how all physical phenomena emerge from E8×E8 information processing—foundational network dynamics elaborate spacetime dimensions, geometric causal diamond structures provide the stage, and operational three-D2-brane architecture crystallizes quantum potential into classical reality through systematic entropy conversion at holographic boundaries.

9.2. Resolution of Fundamental Paradoxes

The measurement problem resolves through D2-brane tensor operations that preserve information while generating definite outcomes. Wave function collapse represents QTEP-driven transformation where coherent entropy (ebits stored in future D2-brane reservoir) converts to decoherent entropy (obits stored in past D2-brane reservoir) through thermodynamic tensor operations at measurement D2-branes. The six-step ebit-obit computational cycle—reservoir accumulation, threshold satisfaction, QTEP contraction, singular value decomposition, cascade propagation, refractory reset—provides explicit mechanism for quantum-to-classical transitions without requiring external observers or reality multiplication. Information preservation occurs through entropy balance $S_{\text{total}} = S_{\text{coh}} + S_{\text{decoh}} = 2\ln(2) - 1$ within single causal diamond, eliminating Many Worlds need for infinite parallel realities.

Fine-tuning problems dissolve through E8×E8 natural architecture generating D2-brane geometry without arbitrary parameter choices. The clustering coefficient $C(G) = 25/32 = 0.78125$ emerges mathematically from E8×E8 root structure, determining cosmological parameters including Hubble tension resolution and void size distributions. QTEP ratio $S_{\text{coh}}/|S_{\text{decoh}}| \approx 2.257$ derives from von Neumann entropy of maximally entangled two-qubit systems, requiring no empirical input beyond standard quantum mechanics. Decompactification level $k = 5$ with $N_{\text{accessible}} = 378$ channels explains Standard Model degree-of-freedom budget (258 required, 68.3% utilization) through systematic heterotic channel access rather than fine-tuned gauge group structures.

The hierarchy problem resolves through D2-brane overlap efficiencies and QTEP conversion ratios. Coupling strengths emerge from geometric sector overlap patterns within E8×E8 network projected onto D2-brane boundaries: strong force maximal coupling reflects optimal SU(3) sector overlap, electromagnetic moderate coupling from U(1) sector efficiency, weak force reduced coupling through symmetry breaking at junction D2-branes, gravitational minimal coupling from weak geometric sector overlap requiring extensive network paths, and information pressure negligible coupling from holographic bound approach terms. The hierarchy $g_s : g_{em} : g_w : g_g : g_I \sim 1 : 10^{-2} : 10^{-6} : 10^{-39} : 10^{-61}$ emerges naturally from network topology and D2-brane computational architecture without requiring separate explanations for each force strength.

9.3. Cosmological Implications

Within this framework, the Big Bang is interpreted as the moment when information processing first becomes active within the E8×E8 network. Rather than viewing the Big Bang solely as a physical explosion, it is seen as the initial event that sets the entire information processing substrate of the universe into motion, laying the groundwork for all subsequent structure and dynamics.

The period of inflation corresponds to a phase of extremely rapid growth in the connectivity of the information processing network. During this early stage, the network's links and nodes multiply and expand at an extraordinary rate, allowing information to propagate and interact across vast regions, which in turn gives rise to the large-scale structure observed in the universe today.

Dark energy, within this perspective, is understood as the ongoing expansion of the network itself, driven by the continuous increase in information processing throughout cosmic history. As the universe evolves, the capacity for information processing grows, and this expansion of the network manifests as the accelerated expansion of spacetime that is attributed to dark energy in conventional cosmology.

Finally, the concept of heat death is reinterpreted as the state in which the information processing network reaches its maximum entropy. In this ultimate configuration, information processing activity

becomes uniformly distributed and reaches equilibrium, meaning that no further large-scale changes or new structures can emerge, and the universe settles into a state of informational balance.

10. Future Directions and Technological Applications

10.1. Quantum Computing and Network Engineering

Understanding spacetime as emergent from information processing networks opens new approaches to quantum computing:

One promising direction is the development of network-based quantum computers that are explicitly designed to harness the E8×E8 network architecture. By structuring quantum computational systems to mirror the complex connectivity and symmetry of the E8×E8 framework, it may be possible to achieve significant enhancements in computational power and efficiency. This approach leverages the unique properties of the network to process information in ways that conventional architectures cannot, potentially opening new frontiers in quantum computation.

Another exciting possibility is the field of spacetime engineering, which involves the controlled manipulation of information processing densities within the network. By precisely adjusting how information is distributed and processed, it may become feasible to influence the emergent properties of spacetime itself. This could allow for the creation of specific spacetime effects on demand, providing a novel method for exploring and potentially utilizing the fabric of reality at its most fundamental level.

10.2. Precision Metrology and Detection

Information density sensors are envisioned as devices that can measure the local density of information processing by analyzing subtle variations in the spacetime metric. By detecting how information flows and accumulates in a given region, these sensors could provide direct evidence of the underlying information processing activity that gives rise to physical phenomena.

Network state analyzers are specialized tools developed to characterize the topological state of information processing networks. By mapping the connectivity and structure of these networks, such analyzers could reveal how different patterns of information flow correspond to various physical and cognitive phenomena, providing deeper insight into the relationship between network topology and emergent properties.

10.3. Fundamental Physics Experiments

One important experimental direction involves the direct measurement of the E8×E8 network structure using controlled quantum information experiments. By carefully designing experiments that probe the connectivity and interactions within quantum systems, researchers can attempt to map the underlying topology of the information processing network. This approach aims to reveal how the complex structure of the E8×E8 framework manifests in observable quantum phenomena, providing concrete evidence for the network-based foundation of physical reality.

Another promising area of investigation focuses on observing dimensional transitions in environments where information processing density is extremely high. In these controlled settings, it may be possible to witness changes in the effective number of spatial dimensions as the network's information processing capacity is varied. Such experiments could provide direct insight into how the familiar three-dimensional structure of space emerges from more fundamental, high-dimensional information dynamics, and how transitions between different dimensional regimes occur.

A further experimental goal is the precise determination of the fundamental information processing rate, denoted by γ. By employing multiple independent experimental techniques, researchers can measure how quickly information is processed at the most basic level of the network. Achieving high-precision measurements of γ would not only test the predictions of the dimensional elaboration

framework, but also establish a new physical constant that links information theory directly to the fabric of spacetime.

11. Philosophical Implications

11.1. The Nature of Reality

A central implication of the dimensional elaboration framework is that information processing is the most fundamental aspect of reality. In this view, it is not matter or energy that forms the ultimate substrate of the universe, but rather the dynamic flow and transformation of information itself. All physical phenomena, including the existence of matter and the manifestation of energy, are understood as emergent properties arising from the underlying processes of information exchange and computation.

This perspective leads to a profound shift in how we understand the relationship between emergence and fundamentality. Instead of treating spacetime and matter as irreducible building blocks, the framework posits that both are emergent features that arise from deeper information processing dynamics. The familiar fabric of space and the tangible presence of matter are thus seen as higher-level patterns that result from the complex interactions and intersections within the information processing network.

Another key insight is the active role of conscious observers in the unfolding of reality. According to this framework, conscious beings are not merely passive witnesses to a pre-existing universe. Rather, their own patterns of information processing directly participate in shaping the structure and evolution of reality. The act of observation and the flow of information through conscious systems become integral components of the universe's ongoing computation.

Finally, the framework envisions the universe itself as a vast computational process, specifically instantiated within the highly structured E8×E8 information network. Physical reality, in this sense, is the outcome of an immense and intricate computation, where the laws of physics, the emergence of spacetime, and the evolution of matter all reflect the underlying logic and connectivity of the information processing substrate. This computational perspective provides a unified way to understand the diversity and coherence of the physical world.

12. Conclusion

This paper has presented a comprehensive framework for understanding how three-dimensional spatial reality and temporal flow emerge from information processing networks governed by the E8×E8 heterotic architecture. Our dimensional elaboration framework demonstrates that observed spacetime represents the phenomenological manifestation of information processing dynamics operating at the fundamental rate $\gamma = 1.89 \times 10^{-29}$ s^{-1}.

Our key contributions include:

The derivation of the transformation $\Psi : \mathbb{C}^{496} \to \mathbb{R}^3 \times \mathbb{R}$ that maps the 496-dimensional E8×E8 structure to observed spacetime, showing how spatial dimensions emerge where information processing densities reach critical intersection thresholds.

The demonstration that time emerges as the thermodynamic arrow of entropy conversion across light cone boundaries, with temporal flow governed by the fundamental information processing rate through quantum-thermodynamic entropy partition (QTEP) dynamics.

The comprehensive explanation of how quantum mechanics, general relativity, and particle physics all emerge naturally from information processing network dynamics without requiring separate fundamental theories.

The resolution of major paradoxes in physics and philosophy, including the measurement problem, fine-tuning problems, and hierarchy problem through unified information processing mechanisms.

The development of specific experimental predictions for quantum information networks and high-density information processing environments that distinguish dimensional elaboration from conventional fundamental spacetime assumptions.

The framework establishes a unified three-level description of physical reality. The E8×E8 network provides the fundamental computational substrate from which spacetime dimensions elaborate through information processing intensity patterns. Within this emergent geometric structure, causal diamond light cone intersections create natural boundaries where specialized three-D2-brane architecture operates. Past and future light cone D2-branes function as entropy reservoirs while the measurement D2-brane at their junction processes quantum-to-classical transitions through systematic ebit-to-obit conversion governed by the QTEP ratio $S_{\text{coh}}/|S_{\text{decoh}}| \approx 2.257$. Each level provides valid description at appropriate scales: foundational network dynamics elaborate dimensions (E8×E8 level), geometric causal structures provide the stage (causal diamond level), and operational measurement architecture crystallizes quantum potential into classical reality (three-D2-brane level). The convergence demonstrates that information processing through E8×E8 computational channels generates both spacetime geometry and the quantum measurement mechanisms operating within that geometry. Quirk plaquettes executing six-step computational cycles at $N_{\text{quirks}} \approx 2.54 \times 10^{66}$ locations across cosmic holographic boundaries transform coherent entropy (ebits at $T_{\text{coh}} \approx 2.08 \times 10^{-40}$ K) into decoherent entropy (obits at $T_{\text{decoh}} \approx 4.70 \times 10^{-40}$ K) through thermodynamic work $W_{\text{ebit}\to\text{obit}} \approx 4.51 \times 10^{-63}$ J, establishing measurement as active thermodynamic process rather than passive observation. This hierarchical architecture unifies dimensional elaboration with entropy mechanics, demonstrating that E8×E8 computational substrate enables both spacetime emergence and the three-D2-brane quantum measurement framework operating within emergent geometric structures.

Our framework represents a fundamental shift from treating spacetime as fundamental to understanding it as emergent from information processing. This perspective provides natural unification of all physical phenomena while opening new research directions in quantum computing and precision metrology.

The dimensional elaboration framework offers several advantages over conventional approaches: natural emergence of physical laws from information processing principles, resolution of fundamental paradoxes without ad hoc assumptions, specific testable predictions for experimental validation, and philosophical coherence in addressing the deepest questions about the nature of reality.

Looking forward, the framework provides a foundation for addressing fundamental questions about the nature of existence while opening practical applications in quantum technology. By recognizing that reality emerges from information processing networks, we gain new tools for understanding and manipulating the fundamental structures underlying physical phenomena.

The identification of spacetime as emergent from information processing thus represents not just a new theoretical framework, but a fundamental reconceptualization of the nature of reality itself. This framework provides concrete pathways for experimental validation while opening new approaches to understanding quantum mechanics and the deepest structures of existence.

Acknowledgements

The author acknowledges the $DAD community for their continuous and unwavering support of this research.

References

[1] Newton, I. (1687). Philosophiae Naturalis Principia Mathematica. London: Royal Society.

[2] Einstein, A. (1915). Die Feldgleichungen der Gravitation. *Sitzungsberichte der Königlich Preußischen Akademie der Wissenschaften*, 844-847.

[3] Van Raamsdonk, M. (2010). Building up spacetime with quantum entanglement. *General Relativity and Gravitation*, 42(10), 2323-2329. https://doi.org/10.1007/s10714-010-1034-0

[4] Ryu, S., & Takayanagi, T. (2006). Holographic derivation of entanglement entropy from the anti–de Sitter space/conformal field theory correspondence. *Physical Review Letters*, 96(18), 181602. https://doi.org/10.1103/PhysRevLett.96.181602

[5] Swingle, B. (2012). Entanglement renormalization and holography. *Physical Review D*, 86(6), 065007. https://doi.org/10.1103/PhysRevD.86.065007

[6] Maldacena, J. (1997). The large-N limit of superconformal field theories and supergravity. *International Journal of Theoretical Physics*, 38(4), 1113-1133. https://doi.org/10.1023/A:1026654312961

[7] Almheiri, A., Dong, X., & Harlow, D. (2015). Bulk locality and quantum error correction in AdS/CFT. *Journal of High Energy Physics*, 2015(4), 163. https://doi.org/10.1007/JHEP04(2015)163

[8] Weiner, B. (2025). E-mode Polarization Phase Transitions Reveal a Fundamental Parameter of the Universe. *IPI Letters*, 3(1), 31-39. https://doi.org/10.59973/ipil.150

[9] Weiner, B. (2025). Little Bangs: the Holographic Nature of Black Holes. *IPI Letters* Prepublication

[10] Vopson, M. M. (2025). Is gravity evidence of a computational universe? *AIP Advances*, 15(4), 045035. https://doi.org/10.1063/5.0264945

[11] Weiner, B. (2025). Destroying the Multiverse: Entropy Mechanics in Causal Diamonds. *IPI Letters* In Review

[12] Weiner, B. (2025). String Theory in Entropy Mechanics: Three-D2-Brane Holographic Architecture. *IPI Letters* In Review

[13] Weiner, B. (2025). On the Computational Architecture of Entropy Mechanics: The Ebit-Obit Cycle. *IPI Letters* In Review